Comparison of iota scan experiments in different experimental campaigns of the Wendelstein 7-X stellarator

T. Andreeva[1], M. Wappl[1], J. Geiger[1], A. Krämer-Flecken[2], S. Bozhenkov[1], N. Chaudhary[1], G. Fuchert[1], M. Grahl[1], M. Hirsch[1], C. Killer[1], S. Mendes[1], C. Nührenberg[1], K. Rahbarnia[1], H. Thomsen[1], V. Winters[1], G. Wurden[3], D. Zhang[1], and W7-X Team

[1] *Max Planck Institute for Plasma Physics, Wendelsteinstr. 1, 17491 Greifswald, Germany*
[2] *Forschungszentrum Jülich GmbH, IFN-1 – Plasma Physics, D-52425 Jülich, Germany*
[3] *Los Alamos National Laboratory, Los Alamos, NM, 87545, USA*

Introduction and overview of W7-X configuration space

Wendelstein 7-X (W7-X) is a modular advanced stellarator, realizing magnetic configurations optimized for fusion-relevant plasma properties [1]. The W7-X magnet system consists of five identical modules, and is designed to allow the realization of a large diversity of magnetic configurations [4], which can be achieved by variation of seven currents of one W7-X half-module, comprising 5 types of independently powered non-planar coils (NPCs) and 2 types of independently powered planar coils (PCs). Fig.1 (left) shows the schematic view of the configuration space of the machine.

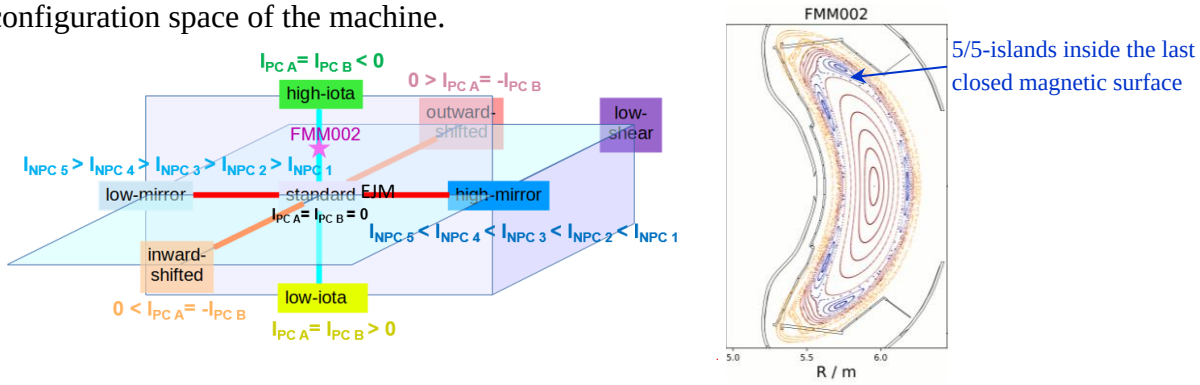

Fig. 1 Left: W7-X configuration space, showing main reference magnetic configurations. Right: Poincaré plot in the so-called bean-shaped poloidal plane, of FMM002 configuration with improved confinement.

Iota scans, performed in the very first experimental campaigns between Standard and High-iota (ST-HI) configurations [2], revealed the confinement improvement in several intermediate limiter configurations, where the plasma volume is restricted by divertor plates intersecting nested flux surfaces. These configurations are characterized by a location of a chain of five magnetic islands inside plasma column, but close to the last closed magnetic surface (Fig.1, right). After these first promising experiments, iota or configuration scans were performed in almost all W7-X experimental campaigns, completing existing findings and expanding them on new parameter range as well as new magnetic configurations. In two latest experimental campaigns similar iota scan discharges were performed in forward and reversed field, in order

to compare confinement properties and analyze a bursty MHD-activity, accompanied confinement improvement in some intermediate limiter configurations, like FMM002 [3].

Confirmation of improved confinement in forward and reversed field experiments

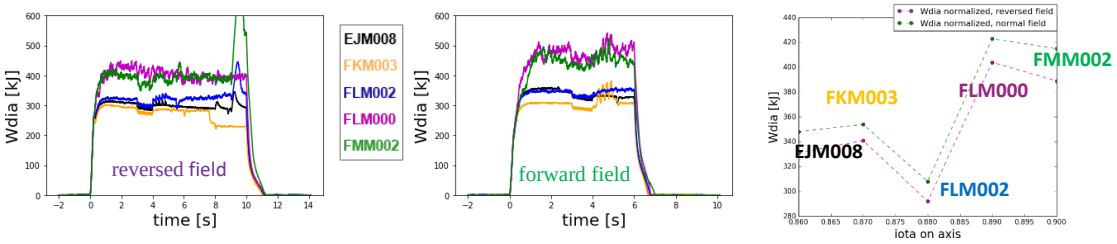

Fig. 2 Left and middle plots: Wdia time traces in comparable discharges in reversed and normal field in a subset of ST-HI scan configurations. Right: Normalized diamagnetic energy in the subset of ST-HI scan configurations.

In the latest W7-X campaign, which was finished in the end of May 2025, a number of discharges in a subset of ST-HI scan configurations were performed at the same parameters as in previously conducted forward field experiments: the targeted ECRH power (P_{ECRH}) was 2 MW and the line-integrated electron density ($\int n_e dl$) was $3.5 \cdot 10^{19}$ m^{-2}. The choice of configurations was motivated by their differences in the magnetic topology and confinement: EJM008 was a starting divertor configuration with $iota_{axis}$~0.86, FKM003 – configuration on a boundary between divertor and limiter cases, $iota_{axis}$~0.87, FLM002 – limiter configuration with standard confinement, $iota_{axis}$~0.88, FLM000 – limiter configuration with so far the best observed confinement, $iota_{axis}$~0.89, FMM002 – another limiter configuration with improved confinement, $iota_{axis}$~0.90, most often conducted in W7-X experiments. Thus one could verify the confinement improvement in reversed field and compare the confinement variation with forward field studies. Fig. 2 (left and middle plots) shows the diamagnetic energy (Wdia) time traces in reversed and forward field experiments, confirming the confinement improvement tendency, reported in [2]. To account for different configuration volumes and slightly different experimental densities, Fig. 2 (right) presents a comparison of the normalized average Wdia, measured between 2.7 s and 3.0 s, scaled to a norm-volume of 31.5 m^3, as well as to a targeted norm-line-density of $3.5 \cdot 10^{19}$ m^{-2}: $\langle Wdia \rangle \cdot (31.5/ V_{Config}) \cdot (3.5 \cdot 10^{19} / \langle n_{e,exp} \rangle)^{\alpha}$ in comparable discharges in reversed and forward field in five different configurations of ST-HI scan. The diamagnetic energy was significantly higher in FLM000 and FMM002 configurations, which well correlates with the previous observations [2].

Comparison of the fluctuations by modification of the island size

The behavior of a bursty MHD-activity, accompanied confinement improvement in some intermediate limiter configurations in previous iota scan experiments, was studied in dynamic

experiments in FMM002 configuration in the latest W7-X experimental campaigns. The increase of currents in control coils (CC) in forward field (or decrease of CC-currents in reversed field) led to the increase of the 5/5-island size in FMM002 configuration. In the middle of the discharge, when CC-currents were reaching their maximum value of 2.5 kA, one can observe a sudden drop in the diamagnetic energy values (see Fig.3, showing time traces of the main dynamic discharge parameters in discussed experiments), accompanied by a vanishing hump in the temperature data (Te) in the outer third of the profiles (Fig.4), being typical for regimes with improved confinement [2]. During this phase of confinement degradation, the amplitude of the bursty MHD-activity flattened. The observations in forward and reversed field experiments with the dynamic increase of the island size correlate well with each other. Experiments with the dynamic reduction of the island size show no major difference in the confinement during the discharge development in both – forward and reversed field discharges. Fig. 4 illustrates the change of plasma profiles in the beginning, in the middle and in the end of the dynamic discharge with island size increasing, corresponding the middle plot in Fig. 3.

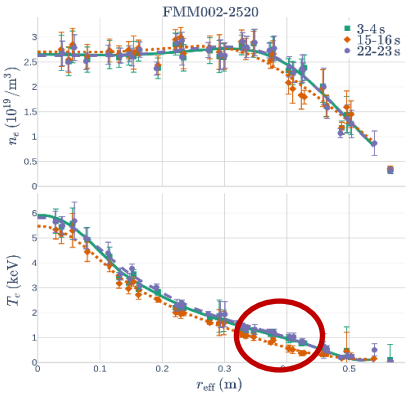

Fig. 4 Density and temperature profiles in the dynamic discharge in reversed field with increasing of island width.

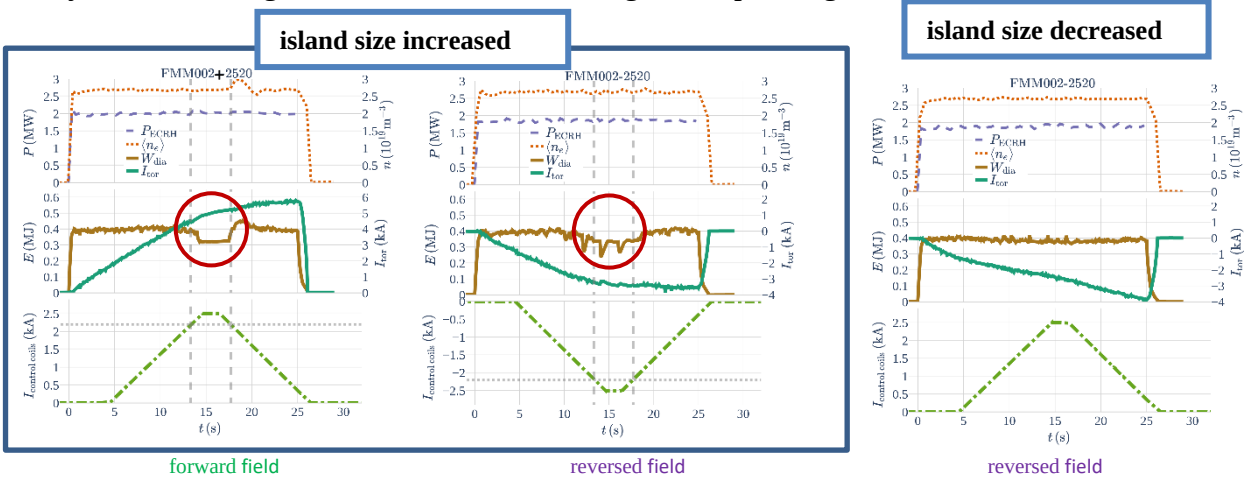

Fig. 3 Left and middle plots: dynamic discharges with increased size of 5/5-islands in forward and reversed field correspondingly. Right: dynamic experiment with the island size reduction in reversed field.

Comparison of detachment programs in normal and reversed field experiments

Further exploration of limiter configurations with improved confinement requires a successful detachment, which was achieved in the latest W7-X experimental campaigns in reversed as well as in forward field experiments. Fig. 5 shows the corresponding time traces as well as bolometry observations in the beginning (2s) of the 2MW discharge with Ne-seeding, middle time point

of the discharge (6s) and in the end of the discharge (10s) with stable detachment. The poloidal asymmetry, seen in the radiation pattern, corresponds findings in [5].

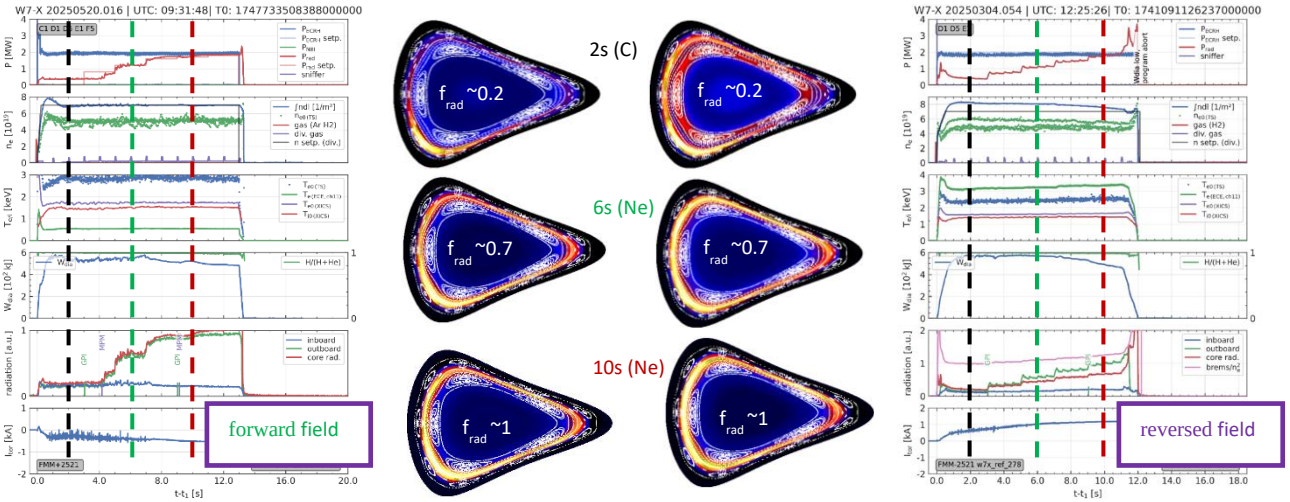

Fig. 5 Comparison of detachment discharges in forward (right) and reversed field (left). The seeding timing scheme was identical in both discharges: 0-3s - no seeding, 3-5s - f_rad=0.4, 5-7s - f_rad=0.6, 7-9s - f_rad=0.8, 9-11s - f_rad=0.85, 11-13s - f_rad=0.9 (in forward field with and in reversed field – without radiation feedback control).

Conclusions

In the latest W7-X experiments in reversed as well as forward field, the confinement improvement was confirmed in some intermediate limiter configurations of Standard-High iota scan. The change of electron temperature profiles in this iota scan corresponds observations in [2]. The behavior of discharges in dynamic experiments with the variation of the island size is similar in both – normal and reversed field experiments. In addition, detachment was successfully realized in the FMM002 configuration with improved confinement in reversed as well as in forward field experiments.

This work has been carried out within the framework of the EUROfusion Consortium, funded by the European Union via the Euratom Research and Training Programme (Grant Agreement No 101052200 — EUROfusion). Views and opinions expressed are however those of the author(s) only and do not necessarily reflect those of the European Union or the European Commission. Neither the European Union nor the European Commission can be held responsible for them.

References:

[1] Grieger G. *et al* 1992 *Fusion Technol.* ***21*** 1767-1778

[2] Andreeva T. *et al* 2022 *Nucl. Fusion.* ***62*** 026032

[3] Wurden G. *et al* Structure of island localized modes in Wendelstein 7-X. *Proc. 46th EPS Conf. Plasma Physics (EPS-2019, Milan Italy) No. P2.1068*

[4] Geiger J. *et al 2015 Plasma Phys. Control. Fusion* ***57*** 014004

[5] *D. Zhang et al 2021 Nucl. Fusion 61 116043*